Turkish Journal of Electrical Engineering & Computer Sciences

http://journals.tubitak.gov.tr/elektrik/

Research Article

Turk J Elec Eng & Comp Sci
(2017) 25: 2322 – 2335

doi:10.3906/elk-1603-279

Dynamic model to predict AC critical flashover voltage of nonuniformly polluted insulators under thermal ionization conditions

Saeed SHAHABI, Ahmad GHOLAMI*
Department of Electrical Engineering, Iran University of Science and Technology, Tehran, Iran

Received: 28.03.2016 • **Accepted/Published Online:** 01.09.2016 • **Final Version:** 29.05.2017

Abstract: This paper presents a theoretical dynamic model based on the Hampton criterion and Mayr's equation for predicting the critical values of flashover on the surface of nonuniformly polluted cap and pin porcelain insulators. The nonuniform pollution layer on the surface of the insulator, the number of disk insulator units, and the geometry of the insulator such as diameter and ribs are the important factors used for prediction. Two types of pollution layer configuration, linear and graded, are introduced as nonuniform pollution layers. The influences of the nonuniform pollution layer on critical flashover voltage are investigated. Furthermore, a random value is added to the surface discharge length during propagation in order to consider the effects of the wind and thermal convection on surface discharge length. The specifications of a real porcelain disk insulator are used in the model. Finally, the estimated results of the proposed model are compared with the measured data of the tests in order to validate the proposed model.

Key words: Ribs, nonuniform pollution, critical flashover voltage, critical resistance, critical leakage current, rate of increase, surface discharge

1. Introduction

One of the major problems for high-voltage (HV) transmission lines is flashover on the surface of polluted insulators. Flashovers caused by pollution are known as temporary faults that can be changed into permanent faults and cause sustained interruption [1].

Over the last decades, researchers and manufacturers have tried to promote mathematical models to overcome the problem of flashover. The first model to predict flashover voltage was proposed by Obenaus. Uniform polluted layers, electric field distribution along the surface of insulator, and the discharge burns in series with the polluted layer were considered under DC voltage [2,3]. Neumarker [4] then presented a modified version of the Obenaus model by using the uniform resistance per unit length of the pollution layer instead of a fixed resistance. Alston and Zoledziowski presented the mechanism of arc extinction by introducing quantitative criteria in terms of electric stress, pollution resistance, and leakage current under DC voltage [5]. Hampton introduced the discharge propagation criterion as a necessary condition for flashover [6]. The mechanism of the discharge reignition process for AC voltage was then analyzed by Rizk [7]. A static model was then developed mathematically to determine the critical condition of flashover [8,9].

Generally, unlike static models, dynamic models are time-dependent. The dynamic behavior of discharge was introduced by Rizk in [10,11]. Mayr's differential equation was used to analyze the discharge performance under AC current. The developed dynamic discharge model presented by Gorur took into account the Hampton

*Correspondence: gholami@iust.ac.ir

criterion, insulator geometry, and surface wettability [12,13]. Dhahabi and Beroual proposed the equivalent impedance of dynamic discharge in series with pollution resistance as a propagation criterion under AC voltage [14]. After that, a developed dynamic model was presented by Aydogmus and Cebeci, in which multiple arcs on the surface of the insulator were considered [15,16]. Further studies were carried out on iced-covered and pollution-covered insulators based on the FEM model [17–19].

In the models proposed by researchers, the nonuniformity of the pollution layer, number of disk insulator units, and wind blowing effects were not considered. In this research, an improved dynamic model of discharge on the surface of polluted insulators will be implemented. The insulator geometry, number of disk insulator units, and nonuniform density of pollution will be considered to predict the AC critical flashover voltage. For validation, the computed results are compared to the minimum flashover voltage measured experimentally on the cap and pin insulator. The results indicate the feasibility of assessing flashover prediction under AC voltage using the proposed model.

2. Review of dynamic surface discharge model

The electrical equivalent impedance of the contaminated surface of insulators will be [14]:

$$Z_{eq}(x) = R_d + \frac{R_p}{1 + j\omega R_p C_p} = \frac{\rho_d x}{S_d} + \frac{\rho_p (L - x)}{S_p(1 + j\omega\rho_p\varepsilon)}, \tag{1}$$

where ρ_p, ρ_d, ε, L, S_p, and S_d are the resistivity of pollution, the resistivity of discharge, the permittivity, the leakage distance of the insulator, the cross-section of the polluted layer, and the cross-section of the discharge channel, respectively. The discharge is assumed a cylindrical channel of radius r and can be described by R_d. The residual impedance of the pollution layer comprises the pollution resistance (R_p) in parallel with the capacitance (C_p) of the pollution layer. According to Dhahbi and Beroual [14], the discharge will propagate if the Hampton criteria as shown in Eq. (2) are satisfied.

$$E_d < \frac{E_p}{\sqrt{a}} \quad E_d < E_p \text{ and } \frac{dZ_{eq}}{dx} < 0 \tag{2}$$

In the above equation, E_d and E_p are electrical strengths of the discharge length and pollution, respectively. Analytical discharge models are based on the equations of fluid dynamics governed by the laws of thermodynamics in combination with Maxwell's equations of electromagnetism theory. Saha's equation is used to describe the degree of ionization in the discharge channel considered as a monatomic gas [20]. Based on the discharge characteristics, the differential equation of the discharge conductance will be:

$$\frac{d\left[\ln g\right]}{dt} = \frac{F'(Q)}{F(Q)}(P_{in} - P_{out}), \tag{3}$$

where g is the momentary discharge conductance, Q is the energy content, F is a function of Q, and Pin and $Pout$ are the power injected to and dissipated by the discharge channel, respectively. The discharge channel is assumed cylindrical and loses its energy by radial heat transfer. Thermal radiation occurs between the discharge channel and the surrounding air. The discharge conductance per unit length can be obtained using Mayr's discharge equation as follows [11]:

$$\frac{dg}{dt} = \frac{1}{\tau}(G - g). \tag{4}$$

In the above equation, G, g, and τ are the steady-state discharge conductance, dynamic discharge conductance, and discharge time constant, respectively.

The pollution layer loses its energy by convection. Joule's first law, also known as the Joule effect, is a physical law expressing the relationship between the heat generated by the current flowing through a conductor [21]. It is expressed as:

$$Q_c = R_p i^2 t, \tag{5}$$

where Q_c is the heat generated by a current i flowing through a pollution for time t. The heat transfer coefficient in thermodynamics is used in calculating the heat transfer, typically by convection between the pollution surface and surroundings.

$$h = \frac{dQ_c/dt}{A.\Delta T} \tag{6}$$

In the above equation, dQ_c/dt is heat flow in input or lost heat flow (J/s), h is the heat transfer coefficient ($W/(m^2K)$), A is the heat transfer surface area (m^2), and ΔT is the temperature difference (K) between the pollution surface and surrounding fluid area. The heat transfer coefficient of air over the pollution surface is assumed to be a constant value of 10 when the speed flow of the air is low [21]. By combining Eqs. (5) and (6), the temperature difference between the surrounding atmosphere and polluted layer on the surface of the insulator can be computed. The change in conductivity with temperature is an important factor that should be considered in the proposed model. The temperature correction (K_σ) of the pollution conductivity at temperature θ (σ_O) can be obtained by the following equation [22,23].

$$\frac{1}{K_\sigma} = \frac{\sigma_{20}}{\sigma_\theta} = \left[3.2\times10^{-8}.\theta^4 - 1.096\times10^{-5}.\theta^2 + 1.0336\times10^{-3}.\theta^2 - 5.1984\times10^{-2}.\theta + 1.7088\right] \tag{7}$$

At every time step, the discharge resistance is calculated by solving Eq. (4). When the propagation criterion is satisfied, the instantaneous velocity of discharge channel propagation will be estimated and then the propagation length can be calculated [14].

3. Nonuniform pollution

In normal conditions, the top and bottom surfaces of suspension disk insulators are polluted independently. The surfaces of insulators are covered by nonuniform pollution. In this study, two types of pollution configurations are analyzed, which are linear nonuniform pollution (Configuration-1) and graded nonuniform pollution (Configuration-2).

3.1. Linear nonuniformity of pollution (Configuration-1)

In industrial regions where the pollution severity is very high and precipitation is low, the maximum pollution thickness (d) takes place near the insulator cap. The linear nonuniform pollution on the surface of a cap and pin insulator is shown in Figure 1. The nonuniform pollution is divided into different sections with the same length (dx_i) and every section is considered as a resistor. Hence, t_i, x_0, x_i, and L are pollution thickness for every section, initial length of the discharge, discharge length, and leakage distance, respectively. The pollution thickness for every section (t_i) and the resistance of each section (R_S) are calculated in Eqs. (8) and (9), respectively:

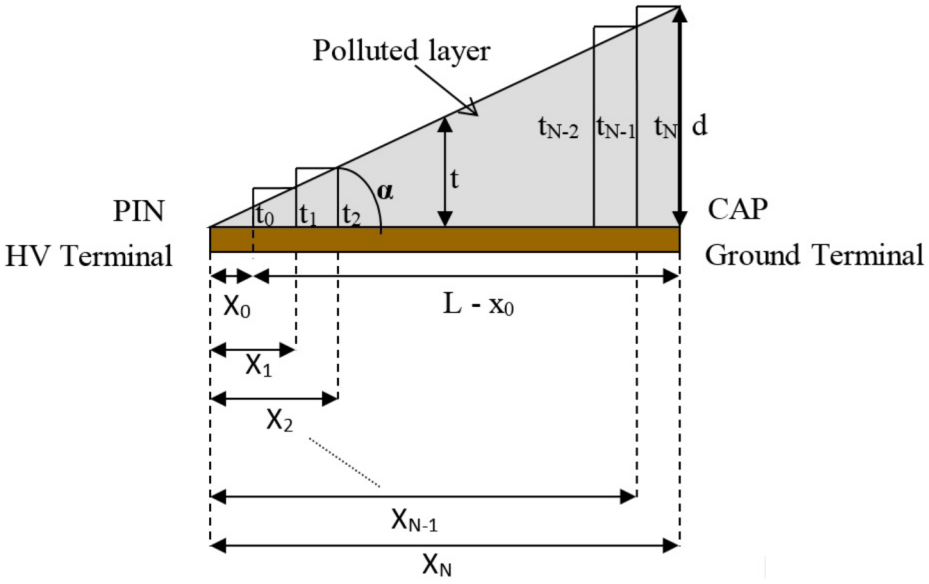

Figure 1. Linear nonuniformly polluted layer of a disk insulator.

$$\tan(\alpha) = \frac{d}{L} = \frac{t_0}{x_0} = \frac{t_1}{x_1} = \ldots = \frac{t_N}{x_N} \rightarrow t_i = \frac{d \times x_i}{L}, \tag{8}$$

$$R_s = \frac{x_{i+1} - x_i}{\sigma.\pi.D_i.t_i} = \frac{x_{i+1} - x_i}{\sigma.\pi.D_i}\left[\frac{L}{d \times x_i}\right] = \frac{(x_{i+1} - x_i).L}{\sigma.\pi.D_i.x_i.d}, \tag{9}$$

where D_i is the diameter of the insulator at every partial leakage distance and σ is the pollution conductivity. By assuming that all of the partial leakage distances are equal to x_0 $(x_{i+1} - -x_i = x_0)$, the total pollution resistance on the surface of the insulator is calculated by:

$$R_{total} = \sum_{i=0}^{M} R_s = \frac{L}{\sigma.\pi.d}\left[\frac{1}{D_0} + \frac{1}{2D_1} + \frac{1}{3D_2} + \ldots + \frac{1}{M.D_{M-1}}\right] = \frac{L}{\sigma.\pi.d}\sum_{i=0}^{M-1}\frac{1}{(i+1)D_i}, \tag{10}$$

where M is the number of sections along the leakage distance and the diameter (D_i) is a function of discharge length. The discharge foot resistance will be added to the pollution resistance. When the propagation criterion is satisfied, the discharge length increases and the pollution resistance decreases by the pollution resistance of the related section.

The analytical model of discharge as shown in Eq. (11) is applied to estimate the critical parameters of flashover on contaminated surfaces of insulators [5]:

$$V = AxI^{-n} + Z_pI, \tag{11}$$

where V is the applied voltage and I is the leakage current, whereas A and n are the characteristic constants of the static discharge. In Eq. (11), x and Z_p are the discharge length and the pollution impedance, respectively. If the pollution layer is only resistive, the derivative of voltage with respect to the current will be applied in the analytical model and then the derived equation will be set to zero as in the following equation.

$$\frac{dV}{dI} = -AxnI^{-n-1} + R_p(x) = 0 \rightarrow I_c = \left[\frac{A.x.n}{R_p(x)}\right]^{1/n+1} \tag{12}$$

By substituting the critical current (I_c) in Eq. (12), the applied voltage will be:

$$V = Ax\left[\frac{A.x.n}{R_p(x)}\right]^{-n/n+1} + R_p(x)\left[\frac{A.x.n}{R_p(x)}\right]^{1/n+1} = (n+1)\left(\frac{R_p(x)}{n}\right)^{n/n+1}(A.x)^{1/n+1}. \quad (13)$$

In Eq. (13), R_p is a function of discharge length. Therefore, by the derivative of the applied voltage (V) in Eq. (13) with respect to the discharge length and setting it equal to zero, we can solve the equation and find the relation between the pollution resistance and the critical discharge length (x_c).

$$\frac{dV}{dx} = 0 \rightarrow \frac{dR_p}{R_p} = -\frac{1}{n}\frac{dx}{x} \rightarrow \frac{R_p(x_c)}{x_c^{-1/n}} = c \rightarrow x_c = \left[\frac{c}{R_p(x_c)}\right]^n \frac{dV}{dx} = A.I^{-n} + \frac{dR_p}{dx}.I = 0 \rightarrow \frac{dR_p}{dx} = -A.I^{-n-1} \quad (14)$$

In Eq. (14), c is a constant value that depends on the applied voltage (V_{ap}) and characteristic constants of the static discharge. The critical value of the discharge length will be obtained by solving this equation. The value of c can be obtained by combining Eqs. (13) and (14):

$$c = nA^{\frac{-1}{n}}\left(\frac{V_{ap}}{n+1}\right)^{\frac{n+1}{n}}. \quad (15)$$

Therefore, by knowing A and n, the critical current will be:

$$I_c = \left[\frac{A.n}{c}\right]^{1/n+1} x_c^{1/n}. \quad (16)$$

As shown in the above equations, the critical values depend on the constant value, c, which is a function of the applied voltage.

3.2. Graded nonuniformity of pollution (Configuration-2)

The pollution severity on the top and bottom surfaces of insulators is in reality often different. Because of this, pollution layers with two different thicknesses are used for this study. As shown in Figure 2, there are two pollution thicknesses on the surface of the insulator. Two states are considered in this configuration of pollution. A higher thickness of pollution covers the top surface and the lower thickness will be on the bottom surface of the insulator in State-1. On the other hand, a higher thickness covers the bottom surface and the top surface is covered by a lower thickness in State-2.

The pollution resistance can be calculated by adding two uniform pollutions with different thicknesses in series with each other. Because of the highest leakage current density at the insulator pin, the dry band starts from the insulator pin and discharge is created and propagates to the insulator cap. The pollution resistance will be:

$$R_p(x) = \begin{cases} r_{p1}L_1 + r_{p2}(L_2 - x) \ ; & x < L_2 \\ r_{p1}(L - x) \ ; & x > L_2 \end{cases}, \quad (17)$$

where r_{p1} and r_{p2} are pollution resistance per unit length of the top and bottom surfaces, respectively. L_1 and L_2 are the top and bottom surface creepage lengths of the insulator, respectively. The discharge length on the

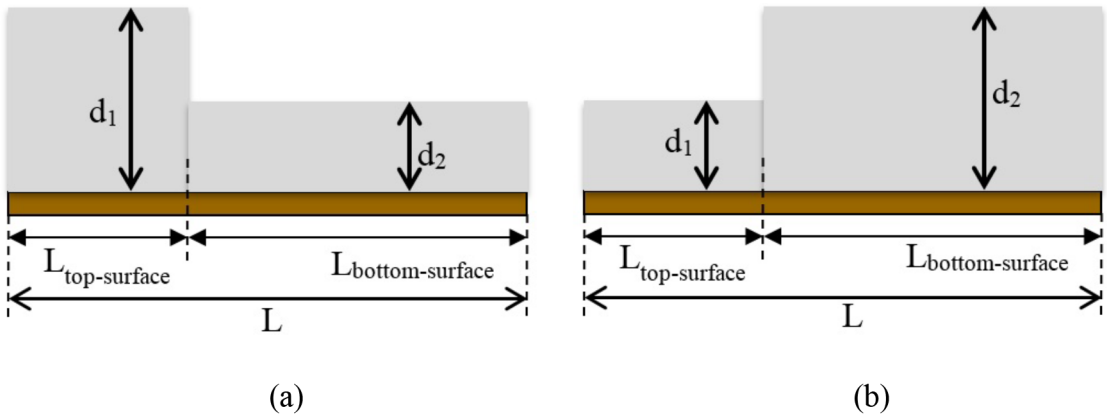

Figure 2. Graded nonuniformly polluted layer: a) State-1 and b) State-2 pollution conditions.

surface is indicated by x in Eq. (17). The critical leakage current of flashover will be the same as obtained in Eq. (12).

By substituting I_c in Eq. (11) and then by derivation of the applied voltage with respect to x and setting it equal to zero, the critical discharge length will be obtained.

$$x_c = \begin{cases} \left(\frac{L_1}{n+1}\right)\left(\frac{r_{p1}-r_{p2}}{r_{p2}}\right) + \frac{L}{n+1} & ;x < L_2 \\ \frac{L}{n+1} & ;x > L_2 \end{cases} \tag{18}$$

As shown in Eq. (18), the critical length of discharge is a function of the pollution resistance of the top surface and bottom surface if the discharge channel is at the bottom surface. When the pollution resistances of the top and bottom surfaces are equal, the critical values will be the same as the uniform pollution critical values.

In both configurations, the open model of the insulator is used in calculations. The diameter of the insulator changes during the propagation of the arc. Accordingly, the discharge current density alters, which results in discharge foot resistance variation.

4. Computational steps

Figure 3 shows the flowchart of the computer program to compute the critical flashover voltage (CFV) of an insulator. The initial conditions of the system such as initial discharge length (x_0), pollution conductivity (σ), pollution configuration, thickness of pollution, insulator geometry, number of ribs (j), ribs' distance from insulator pin ($X_{rib(j)}$), and static discharge characteristic constants are assumed to be known and the different circuit parameters will be calculated. The time step (dt) used in this model is equal to 1 μs, which is suitable for estimating the dynamic discharge conductance. During each step, the electric fields related to the discharge channel and pollution layer, leakage current, pollution resistance, and discharge conductance are calculated. If the propagation criteria are satisfied, the discharge channel will be developed. Otherwise, the peak value of the source voltage will be increased with 100 V and the parameters will be set to their initial values. If the discharge foot is between two ribs (j and $j+1$), the discharge may make a bridge between the ribs. At first it is assumed that the discharge jumps between two ribs. The discharge length is increased by Δx and will be equal to the horizontal distance between rib j and $j+1$ ($X_{hor(j,j+1)}$) together with the leakage distance of rib j from the insulator pin. Thus, $X_{rib(j+1)}$ will be the same as the calculated discharge length. Afterwards, the criteria of

discharge propagation are checked. If they are not satisfied, the discharge length is decreased by Δx and then increased by *dx*, which is related to the discharge velocity. In reality, the pollution discharge channel does not creep exactly on the surface of insulator. The length of dry-band discharge channel is like a curve because of the wind and thermal convection. Therefore, the influences of the wind and thermal convection on the discharge length during propagation are considered as a random value added to the discharge length. The random value is chosen between *0* and Δx or *dx*. However, it is not an accurate evaluation; this type of estimation increases the precision of the model. The program stops when the critical value of the discharge length is reached, so the flashover occurs on the surface of the insulator and the CFV is obtained.

5. Results and discussion

In this study, the LOCKE porcelain insulator (type 20S840) with specifications given in Table 1 is used for investigation. The suspension insulator stringing up to five units of cap and pin insulator are used in this study to obtain the CFV. The two types of pollution configurations explained in the previous sections are used. Critical values such as CFV and critical leakage current (CLC) that are achieved by the proposed model are shown in Tables 2 and 3. In addition, the ratio of critical discharge length (CDL) to total leakage distance (TLD) are calculated and indicated in the tables.

Table 1. Specifications of cap and pin disk insulator.

Characteristic	LOCKE disk insulator
Shed diameter (mm)	254
Cap to pin spacing (mm)	146
Leakage distance (mm)	320
Dry arcing distance (mm)	192

Table 2. The results of proposed model for Configuration-1.

Number of disk Insulators (N)	Conductivity (σ_{25}) [μS/cm]	CFV [kV$_{rms}$]	CLC [A]	$\frac{CDL}{TLD}$
1	20	22.6	0.274	0.72
	80	12.7	0.781	0.72
3	20	112.4	0.100	0.72
	80	68.6	0.258	0.72
5	20	198.7	0.086	0.72
	80	120.9	0.221	0.72

Table 3. The results of proposed model for Configuration-2.

N		State-1			State-2			State-3		
	σ_{25} [μS/cm]	CFV [kV$_{rms}$]	CLC [A]	$\frac{CDL}{TLD}$	CFV [kV$_{rms}$]	CLC [A]	$\frac{CDL}{TLD}$	CFV [kV$_{rms}$]	CLC [A]	$\frac{CDL}{TLD}$
1	20	13.4	0.141	0.494	19.1	0.235	0.806	12.7	0.287	0.568
	80	7.8	0.376	0.494	11.3	0.664	0.806	7.8	0.828	0.568
3	20	36.7	0.328	0.533	38.9	0.544	0.639	32.5	0.444	0.568
	80	21.9	0.840	0.533	23.3	1.424	0.638	19.8	1.198	0.568
5	20	61.5	0.356	0.547	58.0	0.455	0.612	51.6	0.481	0.578
	80	40.3	1.048	0.547	34.6	1.157	0.613	31.1	1.247	0.578

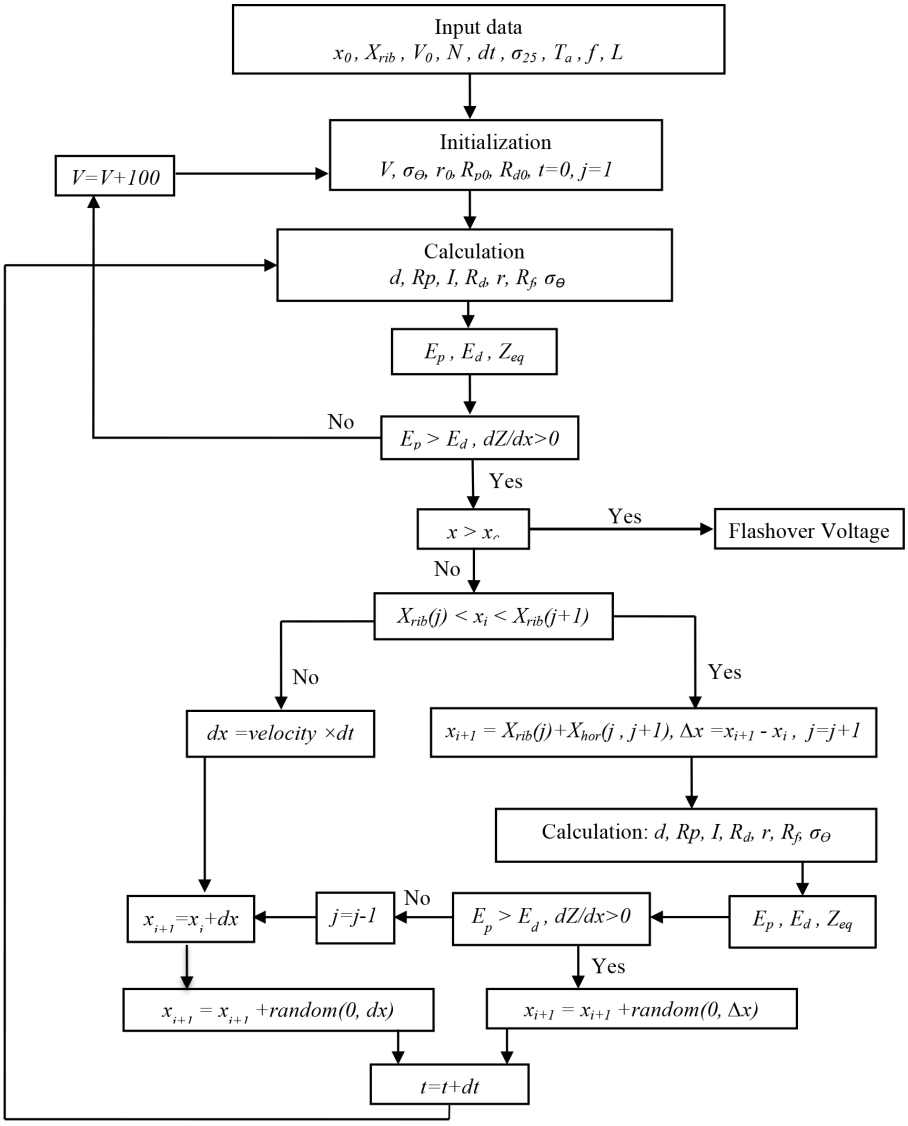

V: applied voltage
X_c: critical leakage distance
d: pollution thickness
r: discharge channel radius
R_f: discharge foot resistance
R_P: pollution resistance
R_d: discharge channel resistance
f: form factor
t: time
dt: time step
I: leakage current
σ_Θ: pollution conductivity
velocity: discharge propagation velocity
T_a: ambient temperature
N: number of disk insulator
L: leakage distance

Figure 3. Flowchart of dynamic flashover model of polluted insulator.

The maximum pollution thickness of 1 cm is used for configuration type 1. As a result, the pollution conductance on the surface of the insulator varies linearly from zero value (HV terminal) to maximum value (ground terminal). As shown in Table 2, the critical discharge length to total leakage distance ratios ($\frac{CDL}{TLD}$) for various conditions have the same value. CFV and CLC values vary from medium (20 μS/cm) to very heavy (80 μS/cm) pollution levels with changing in the number of disk insulator units (N).

In Table 3, three states of pollution distribution for configuration type 2 are considered. Higher and the lower pollution thicknesses of 1 and 0.5 cm are used for State-1 and State-2 as described for Configuration-2. State-3 is related to the uniform pollution distribution. Pollution thicknesses on the top and bottom surfaces are the same and equal to 1 cm. As shown in Table 3, the ratio value ($\frac{CDL}{TLD}$) increases with N for State-1 pollution conditions. On the other hand, the ratio value decreases with N for State-2 pollution conditions. The ratio values of State-3 pollution conditions are almost the same for different numbers of disk units. CFV and CLC values related to State-2 pollution conditions at different pollution conductivities are greater than State-1 pollution conditions when N is less than or equal to three units. In the case of five disk insulators, CFV and CLC values of State-1 pollution conditions are greater than State-2 pollution conditions. Therefore, the bottom surface of the insulator is more serious at low and medium voltage levels. At higher voltage levels, the pollution conductivity on the top surface is more serious.

Figure 4 shows CFV and CLC versus N under standard environmental conditions when the pollution conductivity is 30 μS/cm. In configuration type 1, the maximum pollution thickness of 1 cm is used. In configuration type 2, the higher and the lower pollution thickness are 1 and 0.5 cm, respectively. State-3 is related to the uniform pollution layer on the surface of the insulator, in which the pollution thickness is 1 cm. Figure 4 shows how the configuration of pollution distribution affects CFV and CLC. The CFV level increases with N. The rate of increase of CFV (RICFV) for configuration type 1 of pollution distribution is much more than that of the other type of pollution distribution when N increases. Because of this, the graded nonuniformly polluted layer is more serious than the linear nonuniformly polluted layer at the same level of pollution. It can be observed from Figure 4 that the CLC value related to configuration type 1 of pollution distribution decreases with N. The reason is that RICFV is more than the rate of the rise of pollution resistance, as shown in Figure 5a. However, the CLC graph of uniform pollution conditions rises to the right. The CLC value related to configuration type 2 pollution conditions decreases when N increases from three units to four units. On the other hand, when N increases from four units to five units, the CLC value rises from 731 to 869 mA (State-2). The variation is because of change in discharge foot resistance at the junction of two different pollution thicknesses, as shown in Figure 5b. The discharge foot starts from the bottom surface and then reaches the top surface. When the discharge channel reaches the top surface, the current density changes because of change in pollution thickness that results in alteration of the discharge channel cross-section.

Figure 5 shows the variation of resistance during discharge channel propagation on the surface of the insulator until the flashover occurs. The related critical resistances (R_C), which are dependent on N, are computed and shown in Figure 5. The resistance graphs are the resistance of the pollution layer as well as the discharge foot. As shown in Figure 5a, the rate of increase of critical resistances (R_C) is higher than the related CFV when N increases. Because of this, CLC decreases with N as shown in Figure 4.

The resistance variations of configuration type 2 of pollution distribution (State-2) during discharge propagation on the surface of the insulator are shown in Figure 5b. It can be observed that on a string of insulators consisting of four units ($N = 4$), flashover happens when the discharge channel foot is located at the top surface of the insulator. However, on a string of insulators consisting of two or three units ($N = 2$ or $N = 3$), flashover happens when the discharge channel foot is located at the bottom surface of the insulator. For this reason, the rate of increase of critical resistance (RIR) from three to four units is much higher than the RIR from two to three units. Table 4 shows the RICFV and RIR from two to four disk insulator units. As shown in Table 4, when N increases from three to four units, RICFV will be less than RIR. Therefore, the related CLC decreases when N increases.

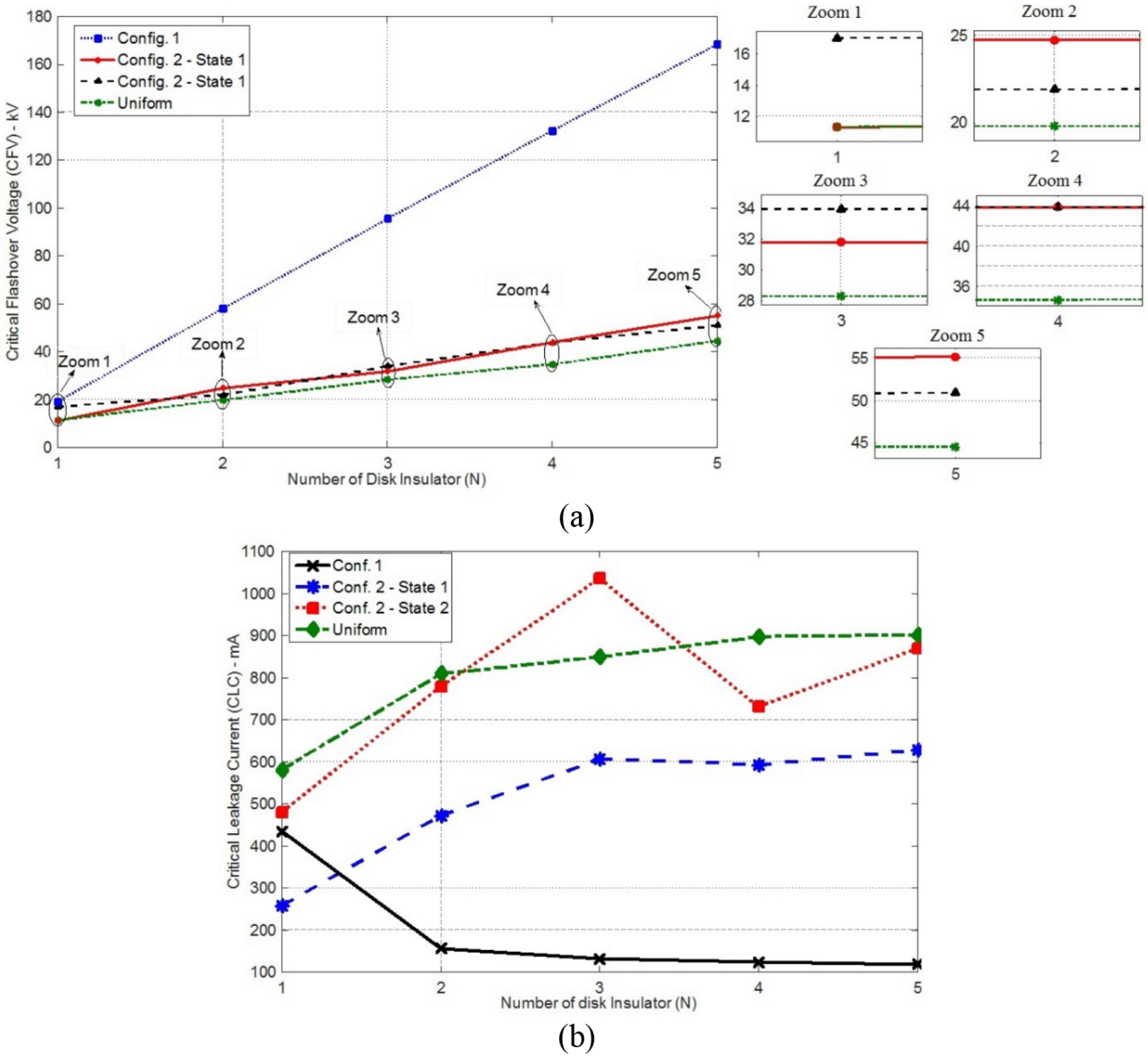

Figure 4. Critical flashover values versus number of disk insulators: a) critical flashover voltage (CFV), b) critical leakage current (CLC).

6. Validation of proposed model

To validate the described model, the results of artificial pollution tests in the HV laboratory at Iran University of Science and Technology are compared with the results obtained from the proposed model. The experimental investigations were carried out in a fog chamber as shown in Figure 6. The transformer used in testing was rated at 50 kV and its short circuit current equals 8 A, complying with IEC standards [23,24]. A salt solution made of sodium chloride (NaCl) and tap water was sprayed on the surface of the insulators uniformly. After the polluted insulators were dried naturally, the top or bottom surface of the polluted insulator would be contaminated again to have a graded nonuniform pollution layer. ESDD (mg/cm^2) was measured after the test according to the IEC standard [24]. The relation between ESDD and surface conductivity (γ_s) is [24]:

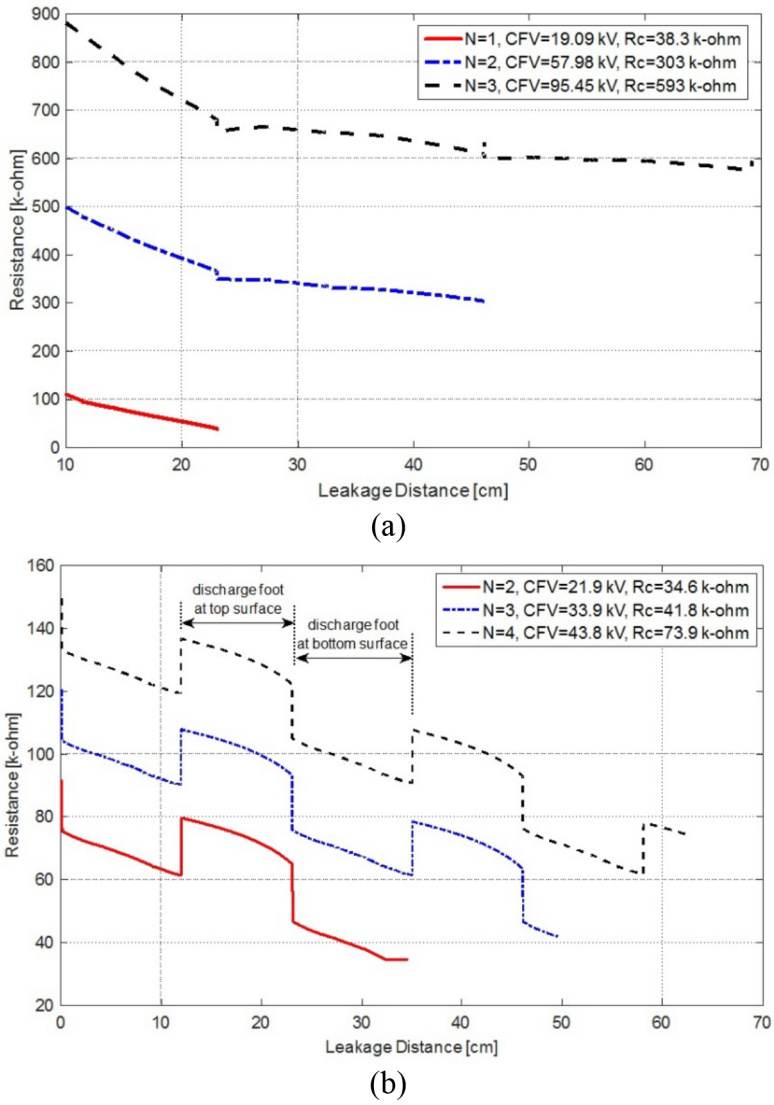

Figure 5. Variation of resistance during discharge propagation on the surface of the insulator: a) configuration type 1, b) configuration type 2 (State-2 polluted layer).

Table 4. Rate of increase of critical flashover voltage and critical resistance for configuration type 2 of pollution distribution.

N	CFV (kV)	RICFV [(1)]	R_C (kΩ)	RIR [(2)]	RICFV and RIR
1	16.97	-	43.4	-	-
2	21.92	4.95	34.6	–8.8	RICFV > RIR
3	33.94	12.01	41.8	7.2	RICFV > RIR
4	43.84	9.9	73.9	32.1	RICFV < RIR
5	50.91	7.07	72.8	–1.1	RICFV > RIR

[(1)] Rate of increase of CFV.
[(2)] Rate of increase of R_C.

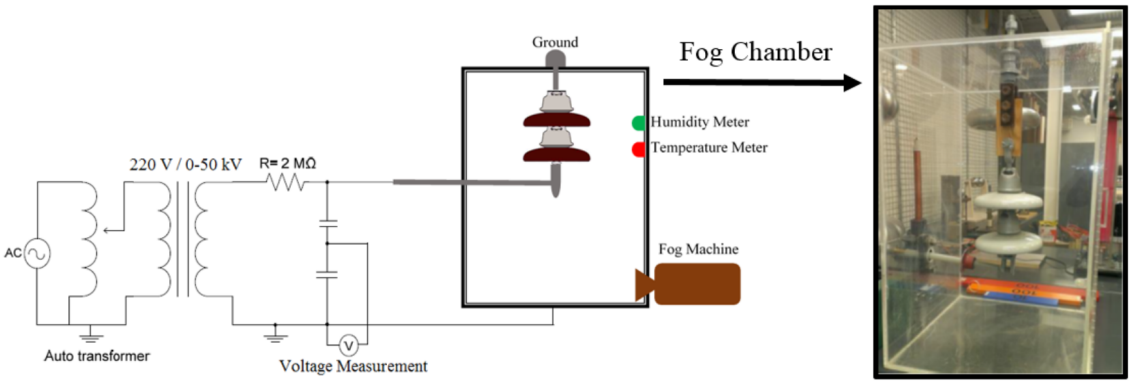

Figure 6. The schematic diagram of test set up and the artificial fog chamber.

$$\gamma_s = (369.05.ESDD + 0.42) \times 10^{-6}. \tag{19}$$

In order to keep the clearance distance between the HV terminal and the chamber glass wall, the insulator string of two disk insulator units was used for experiments. The polluted insulators were wetted by steam fog machine for 20 min until the pollution layer reached maximum conductivity. The test voltage was then applied to the specimen. The pollution flashover voltage was determined according to the up-and-down method [23]. The applied voltage level rises or drops by steps of 5 kV. The results of tests and the proposed model are presented in Table 5. The numerical results achieved by the proposed model are in good agreement with the experimental results.

Table 5. Comparison of experimental results and proposed model results.

ESDD (mg/cm^2), top/bottom		σ (μs/cm), top/bottom	Results (kV$_{rms}$) Proposed model	Lab measurement ($N = 2$)	PMD (%)
S1	0.07/0.03	25.2/11.5	35.3	35	0.85
S2	0.02/0.06	7.8/22.5	37.4	40	6.9
S3	0.12/0.12	44.7/44.7	22.9	25	9.1
ESDD	: Equivalent salt deposit density				
Top	: ESDD at top surface of insulator				
Bottom	: ESDD at bottom surface of insulator				
S1	: State-1 pollution conditions (nonuniform)				
S2	: State-2 pollution conditions (nonuniform)				
S3	: State-3 pollution conditions (uniform)				
σ	: Pollution layer conductivity				
N	: Number of disk insulator units				
PMD	: Proposed model discrepancy				

7. Conclusions

The dynamic model proposed in this paper takes into account the dynamic values of discharge characteristics such as reignition condition, instantaneous changes of discharge length and conductance, and nonuniformity of pollution distribution.

When the pollution conductivity increases, CFV will decrease but CLC will increase. When nonuniform pollution is distributed on the surface linearly (Configuration-1), the ratio value ($\frac{CDL}{TLD}$) will be 0.72, which is

totally independent of conductivity and N. The ratio value ($\frac{CDL}{TLD}$) of State-1 and State-2 pollution conditions (Configuration-2) depends only on N. However, the ratio values of State-3 equal 0.56 for any values of conductivity and N.

The bottom surface of the insulator is more serious at low and medium voltage levels; however, at higher voltage levels, the pollution conductivity on the top surface of the insulator is more serious in comparison to the bottom surface.

The resistance of the discharge channel foot plays an important role in predicting CFV and CLC. The resistance depends on the discharge current density that can be affected by nonuniformity of the pollution distribution.

The CLC of configuration type 1 of pollution distribution depends on the applied voltage, pollution conductivity, and N. The CLC of configuration type 2 of pollution distribution depends on the resistance of the discharge channel foot and leakage current density in addition to the applied voltage, pollution conductivity, and N.

The validation of the model demonstrated that the numerical results of the proposed model for flashover voltages are in good agreement with the experimental results and the discrepancy values are less than 10%, which validates the accuracy of the model.

References

[1] Johns AT, Aggarwal RK, Song YH. Improved techniques for modeling fault arcs on faulted EHV transmission system. IEE P-Gener Transm D 1994; 2: 148-154.

[2] Obenaus F. Contamination flashover and creepage path length. Deustsche Elektrochnik 1958; 12: 135-136.

[3] Boehme H, Obenaus F. Pollution Flashover Tests on Insulators in the Laboratory and in Systems and the Model Concept of Creepage Path Flashover. Paper No. 407. Paris, France: CIGRE, 1966.

[4] Neumarker G. Contamination State and Creepage Path. Berlin, Germany: Deustsche Akad. Wissenschaft.

[5] Alston LL, Zoledziowski S. Growth of discharges on polluted insulators. P IEE 1963; 9: 325-326.

[6] Hampton B. Flashover mechanism of polluted insulation. P IEE 1964; 111: 985-990.

[7] Rizk FAM. Analysis of dielectric recovery with reference to dry zone arc on polluted insulators. In: IEEE PES Winter Power Meeting; 1971. New York, NY, USA: IEEE.

[8] Claverie P. Predetermination of the behavior of the polluted insulators. IEEE T Power Ap Syst 1971; 90: 1902-1908.

[9] Zhicheng G, Renyu Z. Calculation of dc and ac flashover voltage of polluted insulators. IEEE T Electr Insul 1990; 25: 723-729.

[10] Rizk FAM. Mathematical models for pollution flashover. Electra 1981; 78: 71-103.

[11] Mayr O. Beiträge zur Theorie des statischen und des dynamischen Lichtbogens. Archiv fur Elektrotechnik 1943; 37: 588-608 (in German).

[12] Sundararajan R, Gorur RS. Dynamic arc modeling of pollution flashover of insulators under dc voltage. IEEE T Electr Insul 1993; 28: 209-218.

[13] Bo L, Gorur RS. Modeling flashover of AC outdoor insulators under contaminated conditions with dry band formation and arcing. IEEE T Dielect El In 2012; 19: 1037-1043.

[14] Dhahbi N, Beroual A. Flashover dynamic model of polluted insulators under ac voltage. IEEE T Dielect El In 2000; 7: 283-289.

[15] Aydogmus Z, Cebeci M. A new flashover dynamic model of polluted HV insulators. IEEE T Dielect El In 2004; 11: 577-584.

[16] Yawei L, Hao Y, Qiaogen Z, Xiaolei Y, Xinzhe Y, Jun Z. Pollution flashover calculation model based on characteristics of AC partial arc on top and bottom wet-polluted dielectric surfaces. IEEE T Dielect El In 2014; 21: 1735-1746.

[17] Qing Y, Wenxia S, Caixin S, Lichun S, Qin H. Modeling of DC flashover on ice-covered HV insulators based on dynamic electric field analysis. IEEE T Dielect El In 2007; 14: 1418-1426.

[18] Volat C, Farzaneh M, Mhaguen N. Improved FEM models of one- and two-arcs to predict AC critical flashover voltage of ice-covered insulators. IEEE T Dielect El In 2011; 18: 393-400.

[19] Taheri S, Farzaneh M, Fofana I. Dynamic modeling of AC multiple arcs of EHV post station insulators covered with ice. IEEE T Dielect El In 2015; 22: 2214-2223.

[20] Raizer YP. Gas Discharge Physics. Berlin, Germany: Springer, 1991.

[21] Welty JR, Wicks CE, Wilson RE, Rorrer GL. Fundamentals of Momentum, Heat and Mass Transfer. Hoboken, NJ, USA: Wiley, 2008.

[22] Farzaneh M, Chisholm WA. Insulators for Icing and Polluted Environments. Hoboken, NJ, USA: Wiley, 2009.

[23] IEEE. Std. 4. IEEE Standard Techniques for High Voltage Testing. New York, NY, USA: IEEE Press, 2013.

[24] IEC. Std. 60507. Artificial Pollution Tests on HV Insulators to be Used on AC Systems. Geneva, Switzerland: IEC, 1991.